Application of the HEC-RAS Model in Flood Modeling on the Code River Segment in Sewon District, Bantul Regency, Indonesia

Sumunar, A. A. K.,[1] Suprayogi, S.[2*] and Santosa, S. H. M. B.[3]
[1]Coastal and Watershed Management Planning, Universitas Gadjah Mada, Indonesia
E-mail: alvinanindita2000@mail.ugm.ac.id
[2]Department of Environmental Geography, Faculty of Geography, Universitas Gadjah Mada, Indonesia
E-mail: ssuprayogi@ugm.ac.id*
[3]Department of Geography Information Science, Faculty of Geography, Universitas Gadjah Mada, Indonesia
E-mail: sigit.heru.m@ugm.ac.id
**Corresponding Author*

DOI: https://doi.org/10.52939/ijg.v21i2.3929

Abstract
Research on flood hazard and risk mapping has been widely conducted and is crucial for flood disaster management and mitigation. These studies often involve flood modeling using HEC-RAS, which has been applied to major rivers in the Special Region of Yogyakarta Province. This modeling analyses the area and depth of inundation using parameters such as flood hydrographs, Manning's coefficient, and Digital Elevation Model (DEM) data. This study aims to compare the discharge simulated by the GAMA I Synthetic Unit Hydrograph (HSS GAMA I) model with observed discharges using loggers and to evaluate flood modeling with HEC-RAS in Sewon District, Bantul Regency. The results of flood modeling predictions using two different discharge inputs are not too different in terms of discharge and inundation area. Peak discharge values using HSS Gama I are determined as 29.70 m³/s, 52.11 m³/s, and 64.20 m³/s for 2, 5, and 10-year return periods respectively, while values obtained using loggers are 26.16 m³/s, 41.53 m³/s, and 49.56 m³/s. It can be concluded that discharge data from the HSS GAMA I method can still be considered relevant to be used as an alternative method if discharge data is not obtained from direct measurements. Geometry data obtained from the results of aerial photography that is regressed with terrestrial data is also important in this study because it can adjust the basic data and the latest data into one good geometry data. At least the data produced can represent the geometry of the modeled river as closely as possible to the conditions in the field and the results of this study can be a new reference for further research to be able to apply the model and adjust it to the character of each region, so that flood modeling using HEC-RAS becomes more innovative and adaptable to the modeled area.

Keywords: Discharge, Flood, HEC-RAS, Modeling, Code River

1. Introduction

A watershed is an area that receives, stores, and channels precipitation from upstream to downstream through outlets bounded by mountain ridges and valleys [1]. Watersheds invariably face various issues, one of which is flooding. Flooding ranks among the most frequent disasters worldwide, including in Indonesia, and typically occurs during the rainy season. Floods can arise from both natural factors and human activities.

Natural factors contributing to floods include rainfall, river sedimentation, physiography, and river capacity [2]. Similarly, [3] explains that floods result from natural causes or a combination of both natural and human-induced factors. Flooding occurs when water exceeds the capacity of an area to contain or channel it, resulting in physical, social, and economic damage [4]. Insufficient water infiltration can also lead to flooding, especially during heavy and prolonged rainfall. This is influenced by the hydrological cycle, where heavy rainfall increases water levels and river discharge. In addition to rainfall, soil type, land use, and topography also affect flooding. One of the three major rivers in the Special Region of Yogyakarta is The Code River. It flows through three regencies/cities: Sleman Regency in the upstream area, and Yogyakarta City and Bantul Regency downstream. The Code River extends for a total length of 41 kilometers [5].

In Bantul Regency, the river tends to narrow, with natural levees dominated by vegetation, unlike in Yogyakarta City where the levees are mostly artificial and the river has been normalized. Flooding in the Code River's Sewon District has occurred frequently since 2010. One significant cause of these floods is the heavy sedimentation resulting from volcanic mudflows following the 2010 eruption of Mount Merapi. Moreover, the land use around the Code River, primarily residential areas, has reduced water infiltration, exacerbating the effects of the hydrological cycle.

Research on flood hazard and risk mapping has been extensively conducted, particularly in the context of flood disaster management and mitigation efforts as done by [6] who modeled flooding in Jakarta and [7] who conducted the same research in Surat City. The difference in this research is in the use of methods to determine river geometry and its discharge processing. Flood studies are closely associated with flood modeling using HEC-RAS. Flood modeling using HEC-RAS has been widely performed on several major rivers in the Special Region of Yogyakarta Province. This modeling produces visualizations of river water overflow, leading to inundation, which can later be analyzed for area and depth distribution over multiple return periods. This study aims to evaluate the application of the HEC-RAS model in flood modeling to identify its strengths and weaknesses and to analyze the modeling conducted for water resource management purposes.

2. Study Area

The study area is a segment of the Code River located in Bangunhargo Village, Sewon Subdistrict, Bantul Regency. The research covers an area of 70 hectares or 0.7 square kilometers. This river segment spans approximately one kilometer, bordered by earthen embankments with residential areas and rice fields on both sides. This area has faced recurring flooding in recent years. In 2010, flooding alongside the eruption of Mount Merapi, caused sedimentation on the riverbed. In 2015, floods submerged homes, particularly in residential areas such as Pandeyan and Ngoto. Heavy rainfall in 2019 led to the Code River overflowing, resulting in fatalities. In 2022, floods, accompanied by heavy rain and strong winds, caused the collapse of an embankment in Bangunharjo Village and subsequent flooding. Therefore, this location was chosen for the study with the study area boundary depicted in Figure 1.

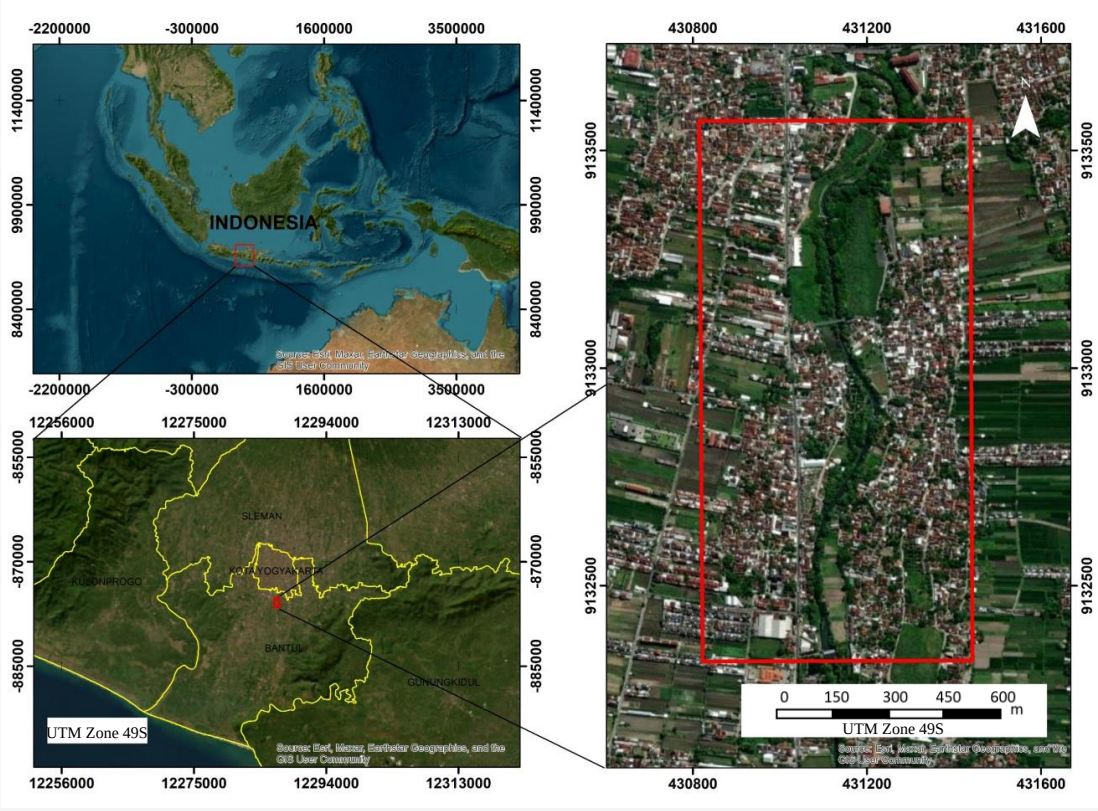

Figure 1: Code river segment in Sewon district, Bantul regency, Indonesia

3. Method

3.1 Data Collection

The research data was categorized into two types: primary data and secondary data. Primary data was collected when secondary data was unavailable or when more detailed information was needed. Secondary data is used to support data processing and validate the primary data. For this study, the availability of secondary data such as rainfall and discharge data was limited to a 10-year period from 2011 to 2020. Cross-sectional existing data and station points were specifically focused on the Code Sub-Watershed. Data collection methods for primary data involved field measurements, specifically referencing aerial photography in this study. Meanwhile, other secondary data types were gathered by requesting information from relevant government institutions. Specific data used in this study was presented in Table 1.

3.2 Rainfall Analysis

Rainfall in the study area was calculated using the Thiessen polygon method. The data used in this calculation included maximum daily rainfall across a span of 10 years. Three station points were utilized to represent the nearest regions around these rainfall stations. The area measurement from the results of the Thiessen polygon method was obtained through processing station point data in ArcMap software.

Frequency analysis was used to estimate design rainfall/discharge for specific return periods. This estimation depended on the chosen distribution type, thus requiring adjustment and selection is determined by the statistical nature of the data. The distribution of rainfall/discharge was determined by sorting statistical parameters from smallest to largest. These parameters include standard deviation (SD), mean ($\bar{X}$), coefficient of skewness (Cs), coefficient of kurtosis (Ck), and coefficient of variation (Cv). The distribution used underwent a goodness-of-fit test, specifically the Chi-Square and Smirnov-Kolgoroc tests [8]. Based on the predetermined distribution type, which in this study was a normal distribution, design rainfall/discharge calculations can be performed using Equation 1:

$$X_T = \bar{X} + K_T \cdot SD \qquad \text{Equation 1}$$

Where:

X_T : Design rainfall for return period T years
$\bar{X}$: Mean value
SD : Standard deviation
K_T : Frequency factor for return period T years

Additionally, rainfall distribution was performed using the Tadashi Tanimoto Method, which distributed rainfall over 8 hours. Effective rainfall was derived from this distribution calculation using the phi index.

Table 1: Data requirements, sources, and outputs for each research objective

Objective	Data	Sources	Outputs
Comparing the discharge of the GAMA I Synthetic Unit Hydrograph (HSS GAMA I) model with the discharge measured using loggers	Rain Gauge Station Locations	Serayu Opak River Basin Development Agency	Synthetic discharge data from GAMA I Synthetic Unit Hydrograph (HSS GAMA I)
	Maximum Daily Rainfall Data (2011-2020)	Serayu Opak River Basin Development Agency	
	Digital Elevation Model (DEM)	DEMNAS (www.tanahair.indonesia.go.id)	
	Watershed Rupa Bumi Indonesia (RBI)	Badan Informasi Geospasial (BIG)	
	Watershed Morphometry	Data Processing	
	AWLR Kaloran Data (2011-2020)	Serayu Opak River Basin Development Agency	Logger-measured discharge data
Evaluating HEC-RAS flood modeling	Digital Terrain Model (DTM)	Aerial Photography	Adjusted river geometry as model input
	Manning's Coefficient	Aerial Photography Interpretation	
	Cross-Sectional Data of Code River	Serayu Opak River Basin Development Agency	

3.3 Discharge Analysis

The flood hydrograph determination in this study used synthetic unit hydrograph HSS GAMA I. This hydrograph was considered suitable for Java Island [9]. HSS GAMA I was tested in 20 watershed areas across Java Island, showing promising results [10]. The design-discharge calculation relied on input data from rainfall distribution and effective rainfall. HSS GAMA I emphasized three crucial aspects for visualizing flood hydrographs: rising limb, peak discharge, and recession. Processing HSS GAMA I data required several parameters from watershed morphometry, which were computed using Equations 2 to 8 as specified in [10].

$$SF = \frac{\sum L_1}{\sum L_i}$$

Equation 2

$$WF = \frac{W_u}{W_L}$$

Equation 3

$$SN = \frac{\sum ST_1}{\sum ST_i}$$

Equation 4

$$RUA = \frac{A_u}{A}$$

Equation 5

$$D = \frac{\sum L_i}{A}$$

Equation 6

$$JN = \sum ST_i - 1$$

Equation 7

$$SIM = WF \cdot RUA$$

Equation 8

Where:

A : Watershed area (km²)
D : Drainage density
L : Main river length (km)
S : River slope
SF: Source factor
SN : Source frequency
WF : Width factor
JN : Number of river junction
SIM : Symmetry factor
RUA : Watershed area factor

After completing the watershed morphometric parameter calculations, the next step involved calculating peak flood discharge (Q_P), peak time (T_P), storage coefficient (K), flood base time (T_B), base flow (Q_B), and recession flow discharge (Q_t). These calculations were performed using Equations 9 to 14. To obtain the Synthetic Unit Hydrograph GAMA I, the value of K was incorporated into the exponential recession curve Equation [10].

$$T_P = 0.43\left(\frac{L}{100}\right)^3 + 1.0665SIM + 1.2775$$

Equation 9

$$Q_P = 0.1836A^{0.58886}TR^{-0.4008}JN^{0.2381}$$

Equation 10

$$T_B = 27.4132TR^{0.1457}S^{-0.0986}SN^{0.7344}RUA^{0.2574}$$

Equation 11

$$K = 0.5617A^{0.1798}S^{-0.1446}SF^{-1.0897}D^{0.0452}$$

Equation 12

$$Q_B = 0.4715A^{0.6444}D^{0.9430}$$

Equation 13

$$Q_t = Q_p e^{-\left(t/K\right)}$$

Equation 14

Observed discharge data was defined as the flow discharge derived from the water level recorded by the AWLR. Each recording station had its calculation formula. In this study, the observed discharge data was taken from the calculations and logger recording at the Kaloran AWLR station. This data was used to compare and evaluate the design discharge results from the HSS GAMA I. A frequency analysis was also conducted on this flow discharge data to determine the discharge for 2, 5, and 10-year return periods.

3.4 Geometry Analysis

The Digital Terrain Model (DTM) was generated from aerial photographs taken using an UAV (Unmanned Aerial Vehicle). In addition to using the DTM, this study also utilized existing cross-sectional geometry data of the river obtained from terrestrial surveys for comparison and correction reference. This was necessary because the geometry data was a crucial input for the HEC-RAS modeling. These two datasets were compared to observe the differences. Aerial photographs were processed with PIX4D software to produce the DTM. The existing cross-sectional data was used as points that contain elevation values. A correlation test was performed after the DTM data values and the existing cross-sections were normally distributed.

Normality was tested using the Kolmogorov-Smirnov method because the dataset contained more than 50 data samples. After the correlation test, subsequent analyses including regression tests, F-tests, and t-tests, were performed. The formulas used were as follows:

$$Y = aX + b$$

Equation 15

Where:

Y: Criterion variable
X: Predictor variable
a : Predictor coefficient
b : Constant/intercept

3.5 HEC-RAS Modeling

The HEC-RAS model was used for hydraulic analysis and was typically utilized for flood inundation mapping. This model was part of the HEC-RAS software. HEC-RAS was developed by the USACE as an application for managing and controlling rivers, channels, ports, and other public works projects. The HEC-RAS software provided simulations for one-dimensional steady flow and two-dimensional unsteady flow, sediment transport, bed calculations, and water temperature/quality modeling [11] [12] and [13]. This modeling was often used for floodplain management and flood safety studies to evaluate flood path distribution [14]. River flow was a process governed by mass conservation and momentum conservation principles. The dynamics and changes in water level and discharge were functions of space and time described by an equation known as the Saint-Venant equation [15]. The Saint-Venant equation consisted of two equations: Equation 16, the continuity equation (mass conservation), and Equation 17, the momentum equation (momentum conservation), which were shown below.

Continuity equation:

$$\frac{\partial A}{\partial t} + \frac{\partial Q}{\partial x} - q_l = 0$$

Equation 16

Momentum equation:

$$\frac{\partial Q}{\partial t} + \frac{\partial QV}{\partial x} + gA\left(\frac{\partial z}{\partial x} + S_f\right) = 0$$

Equation 17

Where:

A : Total cross-sectional area of flow (number of the cross-sectional areas of the main channel and overbank channel) (m^2),
Q : Flow discharge (m^3/s),
q_t : Lateral flow per unit length (m^3/s),
V : Flow velocity (m/s),
g : Acceleration due to gravity (m/s^2),
x : Distance, along the flow direction (m),
z : Water surface elevation (m),
t : Time (s),
S_f : Energy gradient slope (friction slope),
n : Manning's roughness coefficient,
R : Hydraulic radius (m).

3.6 Study Workflow

The peak discharge in this study used two different data, namely the discharge recorded by the logger at the AWLR station and the discharge from HSS GAMA I. Both discharge data were calculated as peak discharge during a specified return period. The results of the two data were used as a comparison and also to evaluate how relevant the results of both were. Furthermore, it was entered into the modeling. The geometric data in this study was DTM data processed from aerial photography with a spatial resolution of 10 cm. The findings of DTM processing were corrected with existing cross-section data. Both data were corrected to obtain the formula used to improve the adjusted DTM data. These results became input data in the modeling. If the modeling has been carried out, a comparison would be made between the two discharges and the results of the flood model from HEC-RAS would be mapped. Study Workflow could be presented in the Figure 2.

4. Result and Discussion

4.1 Rainfall Analysis

The Sub-Watershed Code's catchment area provided the discharge data needed for flood modeling. The total area of the Sub-Watershed Code was 67.247 km^2 and included river flow outlets downstream. Rainfall data was crucial for hydrological analysis. This study utilized maximum daily rainfall data from regular rainfall records from three stations: Prumpung, Kemput, and Gemawang. The rainfall data used covered a 10-year period from 2011 to 2020. The stations were presented in Figure 3. The characteristic of the Sub-Watershed Code was its narrow and elongated shape, resembling a bird's feather [16]. This shape contributed to uneven rainfall distribution due to the limited number of rainfall stations located at only a few points. Therefore, area/regional rainfall calculations were necessary to standardize rainfall across the sub-Watershed Code. The Thiessen Polygon method was employed to estimate precipitation depth. This method assumed that each rainfall station had a linear rainfall variation, and each station point was considered represent its nearest area [17]. The findings were exhibited in Table 2 and Figure 4.

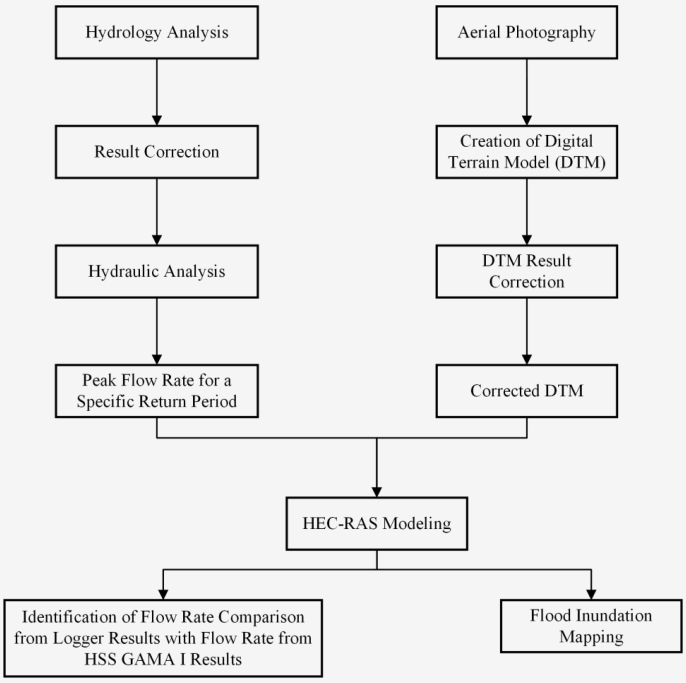

Figure 2: Flood inundation mapping workflow

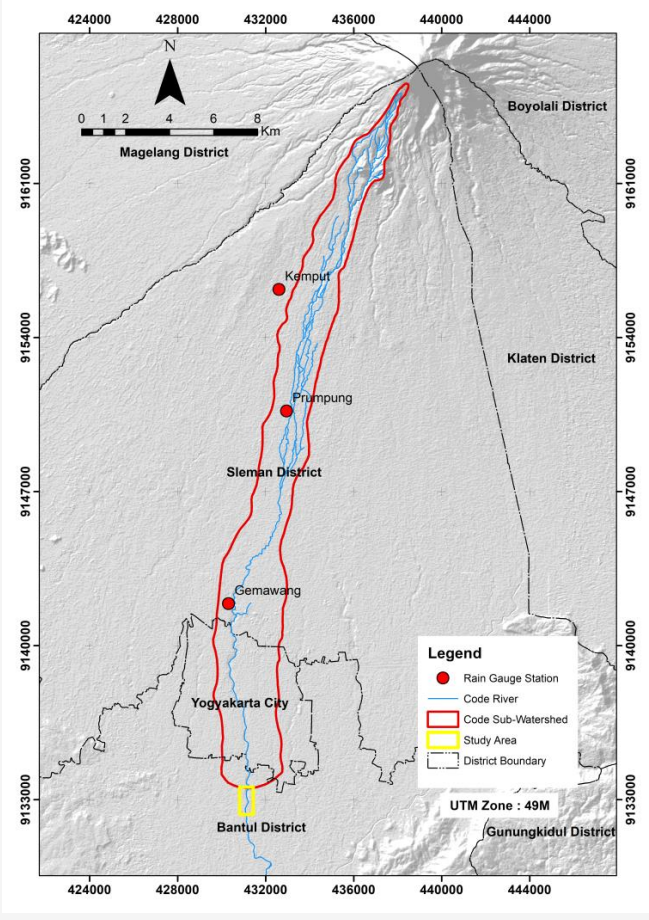

Figure 3: Rain gauge stations

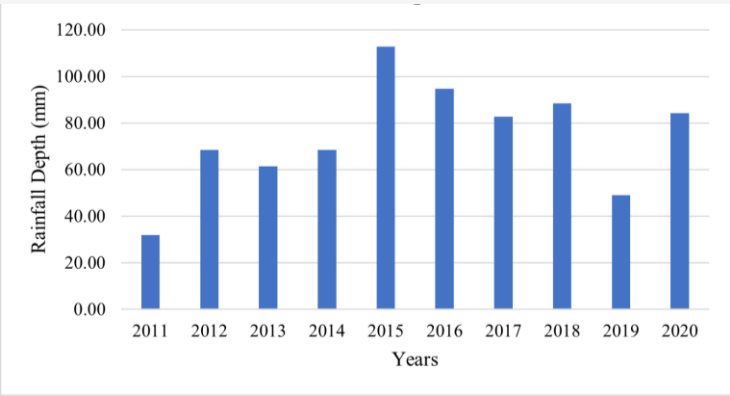

Figure 4: Rainfall depth from 2011 to 2020

Table 2: Rainfall depth

Year	Rainfall Depth (mm)
2011	31.89
2012	68.38
2013	61.41
2014	68.47
2015	112.70
2016	94.75
2017	82.62
2018	88.45
2019	49.03
2020	84.28

Table 3: Rainfall return period

Return Period (Years)	Rainfall (mm)
2	74.20
5	93.90
10	104.20

The calculated rainfall depth underwent further analysis to determine design rainfall for specific return periods. Frequency analysis in this study employed a normal distribution, chosen for its suitability. The return periods considered in this frequency analysis were 2,5, and 10 years. The results of these return period calculations were presented in Table 3. The results of the rainfall return period in the frequency analysis represented the total rainfall amount that occurred in a single day. Therefore, it was necessary to calculate the distribution of hourly rainfall. Rainfall distribution could be depicted as variations in rainfall depth over the duration of the rain in the form of a hyetograph. The rainfall distribution used in this study was based on Tadashi Tanimoto Method, who suggested that this method of hourly rainfall distribution could be applied to Java Island. The calculation results of the rainfall distribution pattern by Tadashi Tanimoto Method indicated an increase in rainfall distribution with longer return periods. This related to the occurrence of extreme rainfall events, which increased in intensity as the return period lengthens. The increased values of rainfall distribution occurred with the same probability level as their return periods. This happened because the probability values at each distribution point still followed the distributed design rainfall. The results of this rainfall distribution pattern were presented in Figure 5.

4.2 Discharge Analysis

Flood discharge could be determined using various methods depending on the data availability and the specific needs. This study utilized two different discharge results: the Synthetic Unit Hydrograph GAMA I (HSS GAMA I) and discharge data obtained from the AWLR station of Serayu Opak River Basin Development Agency. These datasets would be compared across return periods of 2, 5, and 10 years. The discharge data from the AWLR station will be served as observational data to evaluate the discharge results from the HSS GAMA I method. The Synthetic Unit Hydrograph GAMA I (HSS GAMA I) was used to obtain unit hydrograph results. In this study, the flood hydrograph was derived by multiplying the unit hydrograph from GAMA I with the rainfall distribution values within the Sub-DAS Code. Based on the calculated component values, the peak discharge (QP) was relatively small. Although the resulting peak discharge is not very high, it still impacted the magnitude of the peak discharge for each return period. The peak discharge for return periods was calculated using HSS GAMA I and the logger data was presented in Table 4.

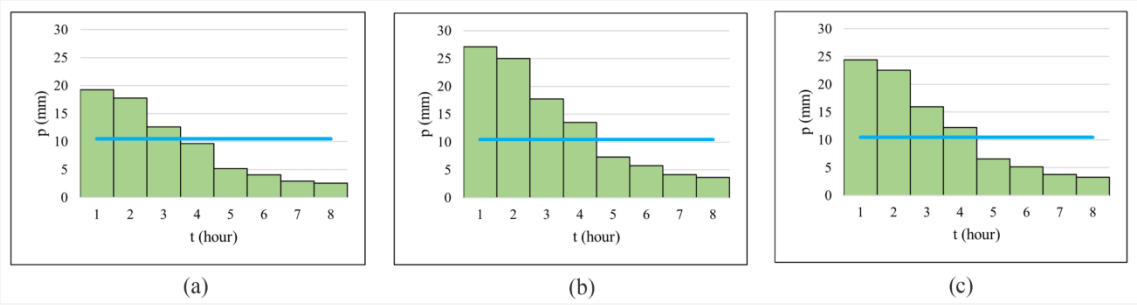

Figure 5: Return period (a) 2 years (b) 5 years and (c) 10 years

Table 4: Discharge return period

Return Period (Years)	Discharge (m³/s)	
	Logger	HSS GAMA I
2	26.16	29.70
5	41.53	52.11
10	49.56	64.20

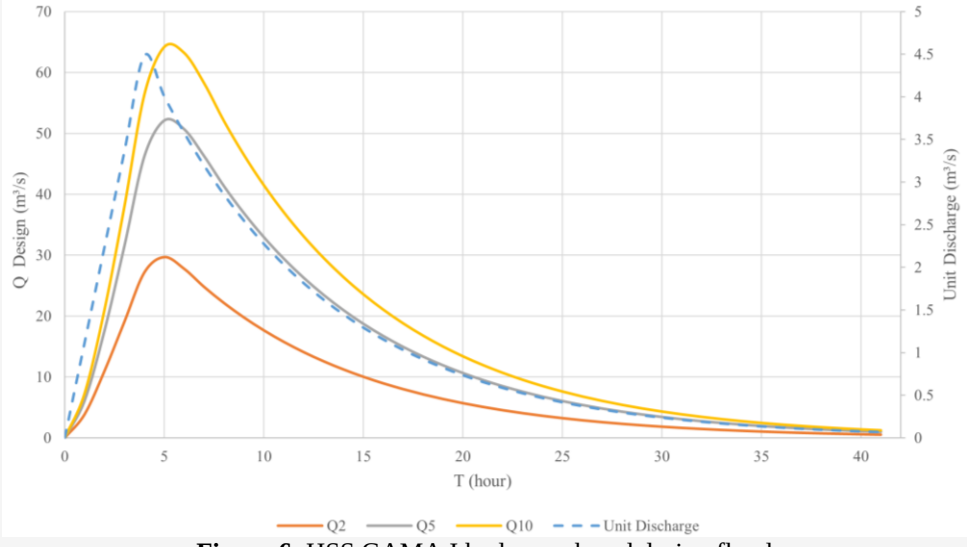

Figure 6: HSS GAMA I hydrograph and design flood

The findings demonstrated that the maximum discharge escalated in direct relation to the duration of the return period. The longer the return period, the greater the peak discharge. The calculation of peak discharge for these return periods assumed that the conditions during the return period were the same as current conditions. The peak discharges for the three return periods differed significantly, especially between the 2-year and 5-year compared to the 5-year and 10-year periods. This was due to the considerable difference in probability between the return periods of 2 years and 5 years, which significantly affected the resulting peak discharge. The design rainfall notably affected the resulting design flood.

Furthermore, the narrow and elongated shape of the sub-watershed caused the hydrograph to reach its peak faster, as rainfall was not well retained and was quickly channelled away. The HSS GAMA I hydrograph and the design flood were presented in Figure 6. The discharges obtained from the model (HSS GAMA-I) are higher than the actual data, and the difference between the model and the logger tends to increase with the length of the return period. This discrepancy should be a primary concern when using the software to model discharge for long return periods. Consequently, fine-tuning of the input parameters is strongly recommended before conducting discharge modeling using HSS GAMA-I model.

4.3 Geometry Analysis

Digital Terrain Model (DTM) data was used as a primary input for HEC-RAS modeling to create river geometry. The available data, in this case, was a DEM sourced from DEMNAS (www.tanahair.indonesia.go.id) at a scale of 1:25,000, which was considered insufficiently detailed for forming accurate river geometry. In this study, DTM data was obtained from aerial photography taken using an UAV in the Code River segment located in Bangunharjo Village, Sewon District, Bantul Regency. The aerial photography was processed into DTM using PIX4D software. This process included filtering to determine ground surface elevation points, sorting, and removing irrelevant objects, which were then interpolated with surrounding elevation data [18] and [19]. Correlation and regression tests were employed to adjust DTM data derived from aerial photography with terrestrial survey data from Serayu Opak River Basin Development Agency. The adjustment began with overlaying cross-section and long-section data from the terrestrial survey onto the DTM from aerial photography. This process involved extracting elevation data from the aerial photography-based DTM adjusted to match the cross-section points from terrestrial survey data.

There were 177 cross-section points from the terrestrial survey data. Before proceeding with correlation and regression tests, a normality test was conducted. The DTM data was referred to as the model, while the terrestrial data was referred to as the field data and were subject to normality testing to determine if their distributions could be considered normal [20]. The results indicated that both datasets were normally distributed. This was because the calculated value which was the maximum value of the absolute difference between the cumulative distribution of empirical data and the cumulative distribution of theoretical distribution was greater than the table value. Likewise, it was conveyed by [21] that the findings from the normality test analysis obtained from the Kolmogorov-Smirnov test produced a calculated value (p-value) that was greater than 0.05 so that it could be concluded that the data was normally distributed.

The normality test results for the model and field data were presented in Table 5.

Table 5: Normality test results

Data	p-Value
Model	0.118
Field	0.163

The data was normally distributed according to the findings of the normality test, allowing for the correlation test to be performed on both datasets. According to Table 6, the correlation test results between the model data and the field data showed a value of 0.507.

Table 6: Correlation test results

Data	Model	Field
Model	1.000	
Field	0.507	1.000

This value was higher than the critical r-value of 0.148 at a 0.05 significance level, indicating that the two datasets were correlated and further analysis could be conducted. According to [22], the analysis could proceed if the r-value was greater than the critical r-value. The subsequent step involved conducting a regression analysis. Regression in this study was used to show the relationship between the independent variable (model data) and the dependent variable (field data). This approach allowed for the examination of changes in the dependent variable based on the independent variable. The results of the regression analysis were presented in Figure 7 and Tables 7-9.

Table 7: Regression model summary

Regression Statistics	
Multiple R	0.744
R Squared	0.553
Adjusted R Squared	0.550
Standard Error	0.617
Observations	177

Table 8: ANOVA

	df	*SS*	*MS*	*F*	*Significance F*
Regression	1	82.913	82.913	217.584	0.00
Residual	176	67.067	0.381		
Total	177	149.980			

Table 9: Regression results

	Coefficients	Standard Error	t Stat	P-value	Lower 95%	Upper 95%	Lower 95.0%	Upper 95.0%
Intercept	29.700	2.578	11.522	0.00	24.613	34.787	24.613	34.787
Model	0.399	0.027	14.751	0.00	0.345	0.452	0.345	0.452

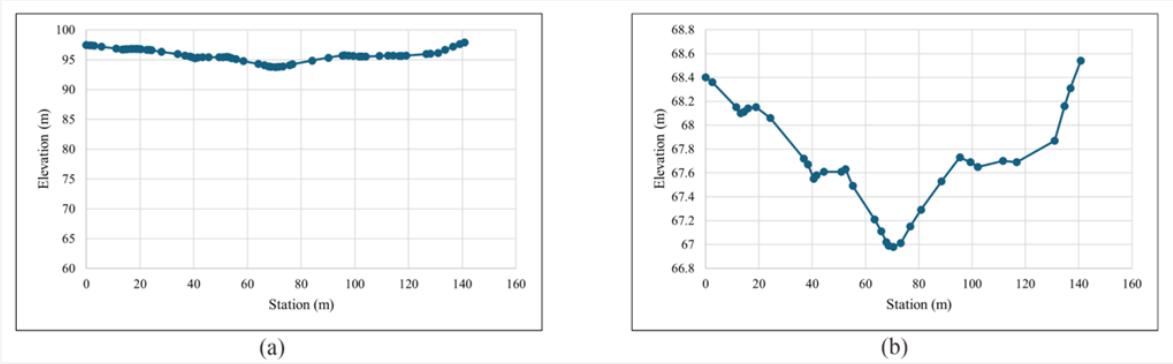

Figure 8: (a) Before adjustment (b) After adjustment

Based on the figures and tables above, the results shown in the ANOVA table indicated that the significance level (F-significance) was less than 0.05, demonstrating that the independent variable significantly affected the dependent variable. In this study, the calculated t-value and the critical t-value were compared using the partial test (T). The critical t-value, with a degree of freedom of df=1 (177-1=176), was 1.973. It was evident that the independent variable significantly affected the dependent variable when compared to the t-value of 14.751. The R^2 value was 55.28%, meaning that the dependent variable (field data) could be explained by the independent variable (model data), with the remaining variance influenced by other factors outside the model data. This was in accordance with the statement [23] A value close to 1 showed that the independent variable provided almost all the information needed to predict the dependent variable, while a value near 0 indicated that the independent variable had very limited predictive power. The adjusted R-Square value ranged from 0 to 1, where a value near 1 suggested that the independent variable offered nearly all the information to predict the dependent variable, and a value close to 0 showed its predictive capability was minimal. According to [22], the correlation in this study was classified as moderate. A moderate correlation between field data and model data indicated a fairly good relationship, but not a very strong one. In this context, although the model data showed similar trends or patterns to the field data, the model's predictions were not always completely accurate or consistent with real conditions.

Because limitations of existing data, Models were often built with certain assumptions or simplifications that did not always reflect the variability of real conditions.

The linear regression equation was derived by incorporating the coefficient (a) and constant (b) values into the regression equation obtained from the analysis. The subsequent step involved incorporating the regression equation into geographic information systems programs to perform geometry calculations (calculate-geometry). This process utilized aerial DTM data as input for the regression equation. While this processing typically did not lead to substantial changes, the adjusted outcomes better aligned better with field conditions. This adjustment aimed to enhance the flood model, particularly its river geometry component, improving overall accuracy and relevance. Thus, these outcomes could better depict a model suitable for disaster mitigation and watershed management reference. The adjusted outcomes are presented in Figure 8.

4.4 HEC-RAS Modeling

The flood modeling results using HEC-RAS included flood inundation distribution and depth. Higher return periods corresponded to increased discharge, influencing both flood depth and the area of inundation modeled. The flood modeling for a 2-year return period using HSS GAMA I and logger data showed relatively similar outcomes. Specifically, HSS GAMA I predicted a discharge of 29.70 m^3/s while the logger data indicated 26.16 m^3/s. The modeled depth also differed only by a few centimeters.

These results were deemed acceptable as the synthetic discharge closely matched the measured discharge for the 2-year return period. During such periods, floods that led to overflow were rare, often resulting in water merely reaching the riverbanks, which were low-lying vacant areas below natural levees.

Period Return periods of 5 and 10 years showed a significant increase in discharge results, followed by deeper flood depths and broader flood distribution. The discharge estimated by HSS GAMA I for the 5-year return period closely matched and slightly exceeded the logger data. Specifically, the 5-year return period discharge from HSS GAMA I was 52.11 m^3/s, while the 5 and 10-year return period discharges from the logger were 41.53 m^3/s and 49.56 m^3/s, respectively. The modeling results for the 10-year return period using HSS GAMA I showed a discharge of 64.20 m^3/s, indicating a significant difference from the logger's discharge. Despite the close alignment between HSS GAMA I and the logger results for the 5-year return period, HSS GAMA I still indicated a higher discharge for the 10-year return period. These findings suggested that there was no significant difference in discharge between the 2-year and 5-year return periods, and the inundation patterns during these periods exhibited substantial similarities. However, there was a noticeable variation in discharge results during the 10-year return period. The difference was also due to the limited length of the data series used as input, which could have influenced the results. When estimating the return period, the length of the data series was highly influential, and in this study, the limited data series likely had some impact on the 10-year return period results. The patterns of flood inundation distribution remained consistent, as the difference in elevation between natural levees and the river water level ranged from 2 to 2.5 meters. Detailed flood modeling results for the 5-year and 10-year return periods were presented in Table 10, and flood inundation distribution could be observed in Figure 9.

Table 10: Flooded area

Data	Inundated area (km^2)		
	2 years	5 years	10 years
Logger	0.033	0.080	0.097
HSS GAMA I	0.038	0.100	0.142

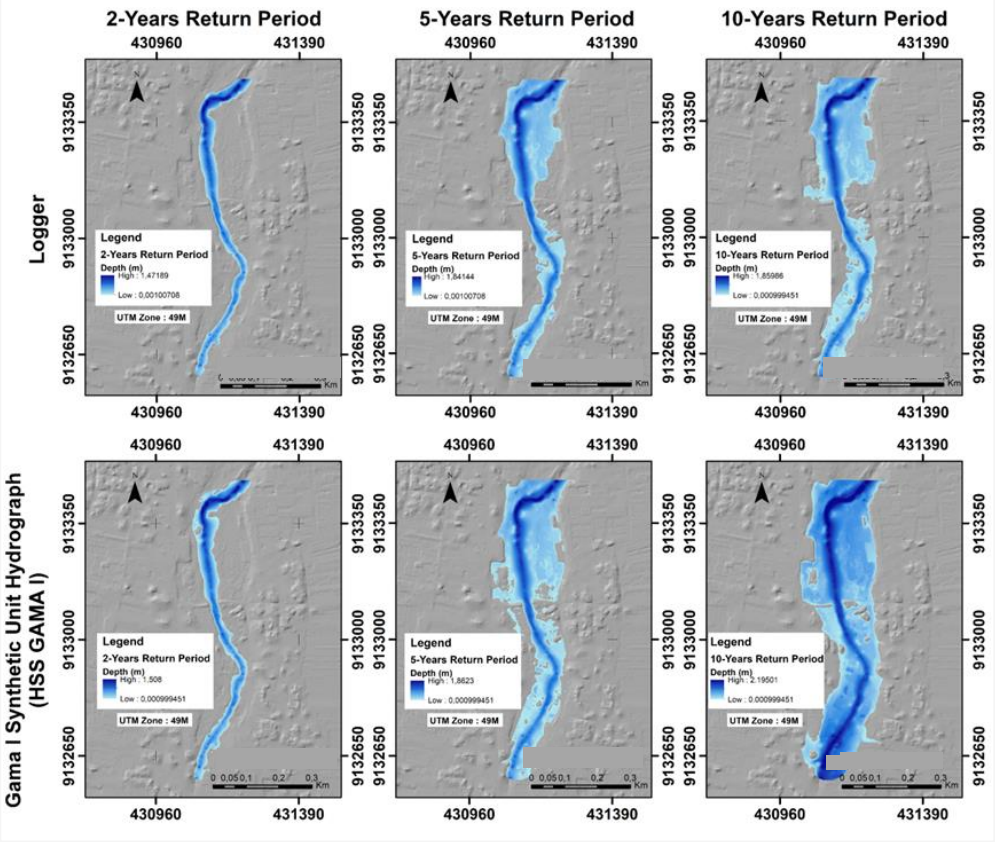

Figure 9: Comparison of flood inundation distribution

The flood characteristics generated from the modeling in this study were not much different from the research conducted by [24] in their case study on flood analysis in the Tigris River. The characteristics of the Tigris Riverbank were similar to those of the Code River, except for differences in depth and river cross-sectional width. Rivers with natural levees, where land use on the banks included settlements and rice fields, had a high risk of flooding. Especially in rivers with dominant meanders, where these bends were almost certain to be affected by flooding. This was also supported by the study conducted by [25], who previously modeled the Baeksan flood event in Korea. In their study, the river section they modeled had meanders, and the results showed that the bends in the meanders were the most affected by flooding. Similarly, the segment of the Code River, which was the focus of the modeling in this study, showed that the upper and middle parts with bends had significantly higher modeling results compared to other points.

5. Conclusion

The results of flood modeling predictions using two different discharge inputs are not too different in terms of discharge and inundation area. It can be concluded that discharge data from the HSS GAMA I method can still be considered relevant to be used as an alternative method if discharge data is not obtained from direct measurements. If you want to predict a longer return period, a longer data series is needed. Geometry data obtained from the results of aerial photography that is regressed with terrestrial data is also important in this study because it can adjust the basic data and the latest data into one good geometry data. It is clear that the difference in geometry data before and after the adjustment is made that although the geometry data in this study can also be said to be imperfect, at least the data produced can represent the geometry of the modeled river as closely as possible to the conditions in the field. The findings of this study may serve as a fresh point of reference for future investigations aimed at applying the model and adjust it to the character of each region, so that flood modeling using HEC-RAS becomes more innovative and adaptable to the modeled area. Although HEC-RAS modeling has long been known and used in various modeling needs, the existence of different methods that are adjusted to the modeled area and provide several innovations and new findings will be something new that can be used as spatial information that can be used as a guideline for compiling regulations or policies related to flood disasters. Trial and error in a study is also needed to get maximum results and can be useful for the government and society in general.

Acknowledgment

The author acknowledges Universitas Gadjah Mada for funding this research through the Final Project Recognition Grant, Universitas Gadjah Mada Number 4971/UN1.P1/PT.01.01/2024 or the RTA Program Universitas Gadjah Mada with Grant Number 5286/UN1.P1/PT.01.03/2024. Thank you also to the Faculty of Geography for holding the fasttrack program from bachelor degree to master degree.

References

[1] Rustika, I., Margana, D. B. and Putro, T. Y., (2018). Sistem Pengukuran dan Pemantauan Ketinggian dan Debit Air Berbasis Mikrokontroler untuk Mendeteksi Potensi Banjir [Microcontroller-Based Water Level and Discharge Measurement and Monitoring System to Detect Potential Floods]. *Proceeding Industrial Research Workshop and National Seminar*, Vol. 9. 57-64.

[2] Seyhan, E., (1990). *Dasar-dasar Hidrologi [Basics of Hydrology]*. Yogyakarta: Gadjah Mada University Press.

[3] Tingsanchali, T. and Keokhumcheng, Y., (2006). Flood Damage Functions for Surrounding Area of Second Bangkok International Airport. *Proceedings, International Symposium on Urban Safety of Mega Cities in Asia, Phuket, Thailand, November*, 291-300.

[4] Rahayu, (2009). *Banjir dan Upaya Penanggulangannya [Floods and Mitigation Efforts*]. Bandung: Pusat Mitigasi Bencana [Disaster Mitigation Center] (PMB-ITB).

[5] BPLH, (2014). *Laporan SLHD Kota Yogyakarta [Yogyakarta City SLHD Report]*. Yogyakarta: Pemerintah Kota Yogyakarta [Yogyakarta City Government].

[6] Afrianto, Y., Marfai, M. and Hadi, M., (2016). Pemodelan Bahaya Banjir dan Analisis Risiko Banjir Studi Kasus: Kerusakan Tanggul Kanal Banjir Barat Jakarta Tahun 2013 [Flood Hazard Modeling and Flood Risk Analysis Case Study: West Jakarta Flood Canal Embankment Damage in 2013]. *Majalah Geografi Indonesia*, Vol. 29(1), 95-110. https://doi.org/10.22146/mgi.13108.

[7] Patel, D. P., Ramirez, J. A., Srivastava, P. K., Bray, M. and Han, D., (2017). Assessment of Flood Inundation Mapping of Surat City by Coupled 1D/2D Hydrodynamic Modeling: A Case Application of the New HEC-RAS 5. *Natural Hazards*, Vol. 89(1), 93–130. https://doi.org/10.1007/s11069-017-2956-6.

[8] Triadmodjo, B., (2008). *Hidrologi Terapan [Applied Hydrology]*. Yogyakarta: Beta Offset.

[9] Marthina, S., Rapar, E., Mananoma, T., Wuisan, E. M. and Binilang, A., (2014). Analisis Debit Banjir Sungai Tondano Menggunakan Metode HSS Gama I dan HSS Limantara [Analysis of Tondano River Flood Discharge Using HSS Gama I and HSS Limantara Methods]. *Jurnal Sipil Statik*, Vol. 2(1), 13-21. https://ejournal.unsrat.ac.id/v2/index.php/jss/article/view/3917.

[10] Harto, S., (2000). *Hidrologi - Teori, Masalah, Penyelesaian [Hydrology - Theory, Problems, Solutions]*. Yogyakarta: Nafiri Offset.

[11] Seker, D. Z., Kabdasli, S. and Rudvan, B., (2003). Risk Assessment of a Dam-Break Using GIS Technology. *Water Science and Technology*, Vol. 48(10), 89-95. https://doi.org/10.2166/wst.2003.0546.

[12] Ngo, A., Grivel, S., Nguyen, T. and Nguyen, T. (2023). Impact Assessment of Land Use and Land Cover Change on the Runoff Changes on the Historical Flood Events in the Laigiang River Basin of the South Central Coast Vietnam. *International Journal of Geoinformatics*, Vol. 19(10), 51–63. https://doi.org/10.52939/ijg.v19i9.2881.

[13] Vojtek, M., Petroselli, A., Vojteková, J. and Asgharinia, S., (2019). Flood Inundation Mapping in Small and Ungauged Basins: Sensitivity Analysis Using the EBA4SUB And HEC-RAS Modeling Approach. *Hydrology Research*, Vol. 50(4), 1002–1019. https://doi.org/10.2166/nh.2019.163.

[14] Shahiriparsa, A., Noori, M., Heydari, M. and Rashidi, M., (2016). Floodplain Zoning Simulation by Using HEC-RAS and CCHE2D Models in the Sungai Maka River. *Air, Soil and Water Research*, Vol. 9, 55–62. https://doi.org/10.4137/ASWR.S36089.

[15] Istiarto, (2015). *Modul Pelatihan Pemakaian HEC-RAS, Simulasi Aliran 1-Dimensi dengan Bantuan Model Hidrodinamika HEC-RAS [HEC-RAS Usage Training Module, 1-Dimensional Flow Simulation with the Help of HEC-RAS Hydrodynamic Model]*. Yogyakarta: MTPBA FT UGM.

[16] Sosrodarsono and Takeda, (2003). *Hidrologi Untuk Pengairan [Hydrology for Irrigation]*. Jakarta: Pradna Paramita.

[17] Suripin, (2004). *Pengembangan Sistem Drainase yang Berkelanjutan [Sustainable Drainage System Development]*. Yogyakarta: Andi Offset.

[18] Perko, R., Raggam, H., Gutjahr, K. H. and Schardt, M., (2015). Advanced DTM Generation from Very High-Resolution Satellite Stereo Images. *ISPRS Annals of Photogrammetry, Remote Sensing and Spatial Information Sciences*, Vol. II-3/W4, 165-172. https://doi.org/10.5194/isprsannals-II-3-W4-165-2015.

[19] Meiarti, R., Seto, T. and Sartohadi, J., (2019). Uji Akurasi Hasil Teknologi Pesawat Udara Tanpa Awak (Unmanned Aerial Vehicle) dalam Aplikasi Pemetaan Kebencanaan Kepesisiran [Accuracy Test of Unmanned Aerial Vehicle Technology Results in Coastal Disaster Mapping Applications]. *Jurnal Geografi, Edukasi dan Lingkungan (JGEL)*, Vol. 3(1). https://doi.org/10.29405/jgel.v3i1.2987.

[20] Budiwanto, S., (2017). Metode Statistika [Statistical Methods]. Malang: Universitas Negeri Malang.

[21] Quraisy, A., (2020). Normalitas Data Menggunakan Uji Kolmogorov-Smirnov dan Shapiro-Wilk (Studi Kasus Penghasilan Orang Tua Mahasiswa Prodi Pendidikan Matematika Unismuh Makassar) [Data Normality Using Kolmogorov-Smirnov and Shapiro-Wilk Tests (Case Study of Parents' Income of Mathematics Education Study Program Students, Unismuh Makassar)]. *J-HEST: Journal of Health, Education, Economics, Science, and Technology*, Vol. 3(1), 7-11.

[22] Sugiyono, (2008). M*etode Penelitian: Pendekatan Kuantitatif, Kualitatif, dan R&D [Research Methods: Quantitative, Qualitative, and R&D Approaches]*. Bandung: Alfabeta.

[23] Ghozali, I., (2018). *Aplikasi Analisis Multivariate dengan Program IBM SPSS 25 (9th ed.) [Multivariate Analysis Applications with IBM SPSS 25 Program (9th ed.)]*. Semarang: Badan Penerbit Universitas Diponegoro.

[24] Ogras, S. and Onen, F., (2020). Flood Analysis with HEC-RAS: A Case Study of Tigris River. *Advances in Civil Engineering*, Vol. 2020, 1-13. https://doi.org/10.1155/2020/6131982.

[25] Dasallas, L., Kim, Y. and An, H., (2019). Case Study of HEC-RAS 1D–2D Coupling Simulation: 2002 Baeksan Flood Event in Korea. *Water*, Vol. 11(10). https://doi.org/10.3390/w11102048.